

Lepton $g - 2$ and W -boson mass anomalies in the DFSZ axion model

Moslem Ahmadvand,^{a,b} and Fazlollah Hajkarim^{c,d,e}

^a*School of Particles and Accelerators, Institute Research in Fundamental Sciences (IPM)
P. O. Box 19395-5531, Tehran, Iran*

^b*School of Physics, Damghan University, Damghan 3671645667, Iran*

^c*Dipartimento di Fisica e Astronomia, Università degli Studi di Padova
Via Marzolo 8, 35131 Padova, Italy*

^d*Istituto Nazionale di Fisica Nucleare (INFN), Sezione di Padova
Via Marzolo 8, 35131 Padova, Italy*

^e*Homer L. Dodge Department of Physics and Astronomy, University of Oklahoma,
Norman, OK 73019, USA*

E-mail: ahmadvand@ipm.ir, fazlollah.hajkarim@pd.infn.it

ABSTRACT: With regard to the leptonic magnetic dipole moment anomaly as well as the W -boson mass excess, we study the DFSZ axion model. Considering theoretical and experimental constraints, we show that the muon and electron $g - 2$ anomalies can be explained within the parameter space of the model for extra Higgs bosons with mass spectra around the electroweak scale and for an almost equivalent contribution of one- and two-loop diagrams. A negative electron $g - 2$ could be achieved by introducing heavy neutrinos. Furthermore, the W -boson mass excess can be consistently addressed within the mass range of the matter content testable at collider experiments.

KEYWORDS: Muon $g - 2$, Electron $g - 2$, W -boson mass, DFSZ axion model

Contents

1	Introduction	1
2	The Model	3
2.1	Physical degrees of freedom in the scalar sector	4
3	Collider constraints	5
4	W-boson mass	6
5	Lepton $g_l - 2$ anomalies	8
5.1	Muon $g_\mu - 2$ anomaly	9
5.2	Electron $g_e - 2$ anomaly	10
5.2.1	Δa_e^{LBK}	11
5.2.2	Δa_e^{B}	12
6	Conclusion	15
A	Minimization and vacuum stability conditions	17
B	Rotations for the Higgs fields	18
C	The mass matrix of neutral scalar fields	19
D	Loop functions	20

1 Introduction

QCD axion models are well-motivated solutions to the strong CP problem of the Standard Model (SM) [1–3]. The axion appears as a pseudo-Nambu Goldstone boson from the spontaneous symmetry breaking of the $U(1)_{\text{PQ}}$ Peccei-Quinn (PQ) symmetry at high temperatures and gains a mass at lower scales around the QCD phase transition [4, 5]. The axion being neutral and long-lived, it is a viable candidate for cold dark matter. It could have been produced in the early universe by the misalignment mechanism or by decays of topological defects [6–9]. A review of different axion models and their cosmological implications can be found in Refs. [10, 11].

Although high-energy experiments have not reported so far any significant deviation from the SM, a set of experiments focusing on precision measurements may indicate anomalies in the SM requiring new physics. One of these high-precision experiments in particle physics measures the muon magnetic moment, $a_\mu \equiv (g_\mu - 2)/2$, where g_μ is the spin g factor

of the muon. Fermi National Accelerator Laboratory (FNAL) has recently reported a large deviation from the SM prediction on a_μ [12], consistent with the previous measurement of Brookhaven National Laboratory (BNL) in 2006 [13]. The result of combining these measurements is

$$\Delta a_\mu \equiv a_\mu^{\text{EXP}} - a_\mu^{\text{SM}} = (251 \pm 59) \times 10^{-11}, \quad (1.1)$$

which shows a 4.2σ discrepancy with the SM prediction [14–34].

Moreover, improved measurements of the fine-structure constant α allow us to extract a value for the electron magnetic moment, a_e , which shows a discrepancy with the SM prediction. Interestingly, there are two experiments whose results on a_e are set in opposite directions. Based on the recoil frequency of ^{133}Cs atoms at Berkeley [35], one has

$$\Delta a_e^{\text{B}} \equiv a_e^{\text{EXP}} - a_e^{\text{SM}} = (-87 \pm 36) \times 10^{-14}, \quad (1.2)$$

which features a 2.4σ discrepancy with the SM prediction [36, 37], while with ^{87}Rb atoms, the result of the Laboratoire Kastler Brossel (LKB) [38] is

$$\Delta a_e^{\text{LKB}} \equiv a_e^{\text{EXP}} - a_e^{\text{SM}} = (48 \pm 30) \times 10^{-14}, \quad (1.3)$$

with a 1.6σ deviation. We emphasize that even if both experiments show tension with respect to the SM in opposite directions, new physics may be required.

Additionally, another precise measured observable is the W -boson mass. Recently, the CDF-II experiment at Fermilab reported a new measurement of the W -boson mass, using data collected from 2002 to 2011 [39]

$$m_W^{\text{CDF-II}} = 80.4335 \pm 0.0094 \text{ GeV}, \quad (1.4)$$

which is in tension with the SM prediction $m_W^{\text{SM}} = 80.357 \pm 0.006 \text{ GeV}$ [40] about 7σ and also differs from the previous average of PDG $m_W^{\text{PDG}} = 80.379 \pm 0.0012 \text{ GeV}$ [40]. Once again, if such a deviation is confirmed, new physics is required.¹

So far, a large number of different scenarios beyond the SM have been proposed to address the anomalies mentioned above (see, for example, Refs. [42–66]). Here, alternatively, we employ the Dine-Fischler-Srednicki-Zhitnitsky (DFSZ) axion model [67, 68], which is an attractive framework that not only addresses the strong CP problem but also provides a viable dark matter candidate. The field content of the model, invariant under the global $U(1)_{\text{PQ}}$, includes a Peccei-Quinn complex scalar field and one additional Higgs doublet. We explore possible explanations for anomalous measurements and their phenomenological implications, restricting the parameter space of the model. Considering vacuum stability and perturbativity conditions as well as collider bounds on the mass of extra Higgs bosons [69, 70], we show that for Higgs fields with masses at the electroweak (EW) scale, the CDF-II W -boson mass anomaly and the anomalous muon magnetic moment can be explained. Furthermore, the measurement of the anomalous electron magnetic

¹Regarding uncertainties that may be originated from hadronic contributions, Ref. [41] demonstrates that the W -boson mass and a_μ anomalies pull the SM hadronic contributions in opposite directions and hence new physics is welcome.

moment can be fitted in the case of a positive contribution. In the case of a negative $g_e - 2$, taking into account the bounds on charged lepton flavor decay processes such as $\mu \rightarrow e \gamma$, extra degrees of freedom (d.o.f.) are required; for example, a heavy neutrino contribution can be added, without spoiling the solutions to the W mass or $g_\mu - 2$.

As we discussed, QCD axion is motivated as a solution to the strong CP problem and can be a candidate for dark matter. These are the low-energy phenomenological consequences of QCD axion models. Depending on the axion model, it can have different kinds of phenomenology at high energies. Here, our focus is on the DFSZ axion model to verify phenomenological effects imposed by possible explanations of the electron and muon magnetic moment and W -boson mass anomaly on the model.

In the next section, we introduce the model and discuss the physical d.o.f. and the mass spectrum. In Section 4, we discuss the oblique parameters, particularly the \mathcal{T} parameter, and its impact on the W mass. Section 5 is devoted to the one- and two-loop-level contributions to the lepton magnetic moment. We conclude in Section 6.

2 The Model

Regarding the smallness of the experimentally bounded CP-violating θ term in strong interactions, i.e. the strong CP problem, several QCD axion models, all based on a $U(1)_{\text{PQ}}$ symmetry, have been proposed. Different QCD axion models correspond to diverse realizations of the PQ symmetry under which the SM is not invariant. In particular, to absorb the θ term, independent chiral transformations of the u and d quarks are required [3]. The model can therefore be enlarged with a second Higgs doublet coupled to only the u - or to the d -quark types via Yukawa interactions [4, 5].

Moreover, the PQ symmetry could be spontaneously broken at an energy scale much higher than the EW scale, leading to the generation of a pseudo-Goldstone boson, the axion. By imposing astrophysical constraints, the symmetry-breaking scale is bounded to $10^8 \text{ GeV} \lesssim f_a \lesssim 10^{17} \text{ GeV}$ [11, 71, 72], where f_a stands for the axion decay constant. This decoupling between the electroweak and PQ symmetry-breaking scales naturally occurs in the presence of a SM-singlet scalar field Φ . This kind of QCD axion model, which has such a field content, is called the DFSZ model.²

The Lagrangian of the model is given by

$$\mathcal{L} \supset \frac{1}{2} |\partial_\mu \Phi|^2 + (D_\mu H_d)^\dagger D^\mu H_d + (D_\mu H_u)^\dagger D^\mu H_u - V(\Phi, H_u, H_d), \quad (2.1)$$

where Φ is the PQ scalar field, H_u and H_d denote the two Higgses, doublets under $SU(2)_L$. The covariant derivative is defined as

$$D_\mu H_{d,u} \equiv \partial_\mu H_{d,u} - i g \tau \cdot W_\mu H_{d,u} - i g' Y B_\mu H_{d,u}, \quad (2.2)$$

where W_μ^a and B_μ are the $SU(2)_L$ and $U(1)_Y$ gauge fields, respectively, whose coupling constants are denoted by g and g' , and τ_i correspond to the Pauli matrices. The scalar

²An alternative approach to the invisible QCD axion is the Kim-Shifman-Vainshtein-Zakharov (KSVZ) model, where in addition to the PQ scalar vector-like quarks are introduced [73, 74].

potential is given by

$$V(\Phi, H_u, H_d) = \lambda_\phi (|\Phi|^2 - V_\phi^2/2)^2 + |H_d|^2 (\kappa_d |\Phi|^2 - \mu_d^2) + |H_u|^2 (\kappa_u |\Phi|^2 - \mu_u^2) - \left(\kappa \Phi H_u^\dagger H_d + \text{H.c.} \right) + \lambda_d |H_d|^4 + \lambda_u |H_u|^4 + \lambda \left(|H_u|^2 |H_d|^2 - |H_u^\dagger H_d|^2 \right). \quad (2.3)$$

Finally, the Yukawa interactions are

$$y_u^{H_u} \bar{Q}_L \tilde{H}_u u_R + y_d^{H_d} \bar{Q}_L H_d d_R + y_l^{H_d} \bar{\Psi}_{L_l} H_d l_R + \text{H.c.} \quad (2.4)$$

where $\tilde{H}_u \equiv -i \tau_2 H_u^*$. The model is invariant under the SM gauge symmetry group $SU(3)_C \otimes SU(2)_L \otimes U(1)_Y$ and under the $U(1)_{\text{PQ}}$, and therefore the PQ charges of the fields in this model can be obtained accordingly [75]. In fact, from the κ term of Eq. (2.3) and the orthogonality between PQ and corresponding hypercharge currents [11], we obtain PQ charges of scalar fields as $X_{H_u} = \cos^2 \beta$, $X_{H_d} = -\sin^2 \beta$, and $X_\Phi = 1$. Moreover, supposing that left-handed fermions have no PQ charges, $X_{u_R} = X_{H_u}$, and $X_{d_R} = X_{l_R} = -X_{H_d}$.

The Higgs doublets can be expanded as [76]

$$H_d = \begin{pmatrix} \alpha_+ \\ \alpha_0 \end{pmatrix} \quad \text{and} \quad H_u = \begin{pmatrix} \beta_+ \\ \beta_0 \end{pmatrix}, \quad (2.5)$$

and their vacuum expectation values (VEV) are given by $\langle \alpha_+ \rangle = \langle \beta_+ \rangle = 0$, $\langle \alpha_0 \rangle = v_d$, $\langle \beta_0 \rangle = v_u$, with $v^2 \equiv v_d^2 + v_u^2$, where $v \simeq 246$ GeV is the EW VEV. Furthermore, $\langle \Phi \rangle = v_\phi \sim f_a$ [11].

Using the minimization of the potential, three parameters μ_d , μ_u , and V_ϕ , can be fixed (see Appendix A); therefore, in the scalar sector, the free parameters are λ_ϕ , $\tan \beta = t_\beta \equiv v_u/v_d$, κ , κ_d , κ_u , λ_u , λ , and v_ϕ . Finally, we note that λ_d is fixed by imposing that one of the Higgs bosons has a mass of 125 GeV, as the SM Higgs.

2.1 Physical degrees of freedom in the scalar sector

In this section, we determine the mass spectrum of the scalar sector. From two complex doublets and a complex singlet, there are 10 d.o.f. Three combined Goldstone components are related to gauge bosons and are eliminated by gauge transformations, corresponding to longitudinal parts of the three massive gauge bosons [76, 77]. After rotating the interaction eigenstates (details of the transformation can be found in Appendix B), the mass eigenstates can be identified. The spectrum counts a pair of charged scalars H^\pm , a pseudoscalar A , three CP-even scalars h_i , and the axion field a .

First, the mass of the pseudoscalar Higgs A is given by

$$m_A^2 = 8 \frac{\kappa}{v_\phi} \left(s_{2\beta} v^2 + \frac{v_\phi^2}{s_{2\beta}} \right). \quad (2.6)$$

From Eq. (2.3), the mass of the charged Higgs fields H^\pm is

$$m_{H^\pm}^2 = 8 \left(\lambda v^2 + \frac{\kappa v_\phi}{s_{2\beta}} \right). \quad (2.7)$$

Furthermore, there are three neutral scalar states, H , S , and ϱ , which are not mass eigenstates and should be expressed in the mass basis where the mass matrix can be diagonalized by a rotation matrix (Appendix C)

$$H = \sum_{i=1}^3 R_{Hi} h_i, \quad S = \sum_{i=1}^3 R_{Si} h_i, \quad \varrho = \sum_{i=1}^3 R_{\rho i} h_i. \quad (2.8)$$

where h_i are mass eigenstates and the rotation matrix, R , and its components are expressed in Appendix C. The mass spectrum of these scalar fields, up to $\mathcal{O}(v^2/v_\phi^2)$, is

$$\begin{aligned} m_{h_1}^2 &\simeq 32 v^2 (\lambda_d c_\beta^4 + \lambda_u s_\beta^4) - \frac{16 v^2}{\lambda_\phi} \left(\kappa_d c_\beta^2 + \kappa_u s_\beta^2 - \frac{\kappa}{v_\phi} s_{2\beta} \right)^2, \\ m_{h_2}^2 &\simeq \frac{8 \kappa}{s_{2\beta}} v_\phi + 8 v^2 s_{2\beta}^2 (\lambda_d + \lambda_u) - 4 v^2 \frac{[(\kappa_d - \kappa_u) s_{2\beta} + 2 \kappa c_{2\beta}/v_\phi]^2}{\lambda_\phi - 2 \kappa/(v_\phi s_{2\beta})}, \\ m_{h_3}^2 &\simeq 4 \lambda_\phi v_\phi^2 + 4 v^2 \frac{[(\kappa_d - \kappa_u) s_{2\beta} + 2 \kappa c_{2\beta}/v_\phi]^2}{\lambda_\phi - 2 \kappa/(v_\phi s_{2\beta})} + \frac{16 v^2}{\lambda_\phi} (\kappa_d c_\beta^2 + \kappa_u s_\beta^2 - \kappa s_{2\beta}/v_\phi)^2. \end{aligned} \quad (2.9)$$

The lighter state h_1 is identified with the SM-like Higgs boson, while h_2 and h_3 are extra heavy neutral CP-even Higgs bosons.

We do not consider cases where the mass spectrum is decoupled from the EW energy scale, but cases that can address the aforementioned anomalous problems and lead to rather light masses for the Higgs fields, phenomenologically interesting for collider physics. In this sense, after fixing t_β , the mass spectrum of the Higgs fields depends mainly on κ , λ , and λ_ϕ . We consider m_{h_1} as the SM Higgs and also fix $\lambda_\phi = 0.01$ that affects m_{h_3} so that the very massive scalar field can be determined close to v_ϕ due to $v_\phi \gg v$.³ The case with $\lambda_\phi \rightarrow 0$ can lead to masses lighter than the SM Higgs mass. SM-like interactions of the Higgs, h_1 , with SM particles can also consistently be obtained, due to the relevant coefficient, a combination of $R_{H1} \sim 1$ and R_{S1} proportional to v^2/v_ϕ^2 , multiplied to SM Higgs couplings. For more details see Ref. [76].

3 Collider constraints

Constraints on the mass spectrum of extra Higgs fields in the framework of the Minimal Supersymmetric Standard Model (MSSM) [78] and two-Higgs-doublet models (2HDMs) [77] are extensively studied [40]. Regarding the mass of the charged Higgs boson, very light masses, $m_{H^\pm} \lesssim 80 \text{ GeV}$ have been excluded by LEP [79] and Tevatron [80]. Moreover, for $m_{H^\pm} < m_t$ (the top quark mass), the experimental lower bound from direct searches is $m_{H^\pm} > 155 \text{ GeV}$ [40]. For mass ranges $m_{H^\pm} \sim 155 - 170 \text{ GeV}$, firm experimental analysis does not exist [81] and a reliable perturbative calculation of the charged Higgs boson production cross section must be performed. For $m_{H^\pm} > m_t$, ATLAS and CMS have also been excluded regions of the parameter space of MSSM, $m_{H^\pm} < 180(1100) \text{ GeV}$, for

³We consider $\lambda_\phi = 0.01$ as a representative value and lighter h_3 can also be obtained for other allowed smaller values of λ_ϕ .

$t_\beta = 10(60)$, with a certain luminosity [40]. This search is sensitive to the modeling of the top pair production background with extra partons and especially b-quarks.

Also, there have been numerous experimental searches at the LHC for a pseudo-scalar boson, excluding light pseudoscalar Higgs bosons $m_A \lesssim m_{h_1}/2$ [70]. In addition, in the context of MSSM, for heavy neutral/pseudo-scalar Higgs bosons in the $\tau\tau$ final state, the exclusion region is $m_A \lesssim 390(1600)$ GeV for $t_\beta = 10(60)$ [40]. However, in the diphoton channel a slight excess has been observed by CMS at a mass of 95.3 GeV, consistent with the observed excess at LEP, with a local significance of 2.8σ and could not be ruled out by ATLAS at 95% CL [40].

Experimental searches including extra Higgs production crucially depend on accurate theoretical predictions for inclusive cross sections. (For instance see Ref. [82] for precise predictions of pseudo-scalar inclusive cross section specially for the moderate mass range.) According to the matter content of our model and its parameter space, given additional decay channels, for instance $H^\pm \rightarrow aW^\pm$, $A \rightarrow ah_1$, $h_2 \rightarrow aa$, and $h_2 \rightarrow aZ$, the bounds may somehow change.⁴ Here, aside from the exclusion region independent from t_β , i.e., $m_{H^\pm} \lesssim 155$ GeV and $m_A \lesssim m_{h_1}/2$, we consider other mass values, provided that the model parameter t_β is in the viable, allowed range. In the following calculations, we show that the anomalies may simultaneously be explained for $t_\beta > 100$.

4 W-boson mass

In this section, we study the effects of new physics on the recently reported W -boson mass excess by analyzing the oblique parameters of this model [83, 84]. Some studies have already considered the impact of having a second Higgs doublet in the W -mass anomaly; see, e.g. Refs. [42, 43, 46, 48, 50, 51, 53–58, 60, 85]. The leading correction to the W -boson mass can be approximated as

$$\Delta m_W^2 \simeq \alpha \frac{c_W^4}{c_W^2 - s_W^2} m_Z^2 \Delta\mathcal{T}, \quad (4.1)$$

where $\Delta\mathcal{T}$ is one of the Peskin-Takeuchi parameters, obtained by the following procedure. The one-loop corrected masses of the gauge bosons are given by

$$m_W^2 \simeq \frac{g^2 v^2}{2} + \Pi_{WW}(0), \quad (4.2)$$

$$m_Z^2 \simeq (g^2 + g'^2) \frac{v^2}{2} + \Pi_{ZZ}(0), \quad (4.3)$$

where $\Pi_{WW}(0)$ and $\Pi_{ZZ}(0)$ are the two-point functions of the gauge fields at zero-momentum transfer [76]. The deviation from the custodial symmetry can be parameterized as

$$\rho \equiv \frac{m_W^2}{m_Z^2 c_W^2} = \frac{m_{W(\text{tree})}^2 + \Pi_{WW}(0)}{m_{Z(\text{tree})}^2 c_W^2 + \Pi_{ZZ}(0) c_W^2} \simeq 1 + \frac{\Pi_{WW}(0)}{m_{W(\text{tree})}^2} - \frac{\Pi_{ZZ}(0)}{m_{Z(\text{tree})}^2}, \quad (4.4)$$

⁴We leave precise cross section calculations to a future work.

where $m_{V(\text{tree})}^2$ is the mass at tree level of the gauge boson V , and

$$\Delta\rho \equiv \frac{\Pi_{WW}(0)}{m_{W(\text{tree})}^2} - \frac{\Pi_{ZZ}(0)}{m_{Z(\text{tree})}^2}. \quad (4.5)$$

Thus, $\Delta\mathcal{T} = \Delta\rho/\alpha$ is [76]

$$\begin{aligned} \Delta\mathcal{T} &= \frac{1}{16\pi s_W^2 m_W^2} \left[m_{H^\pm}^2 - \frac{v_\phi^2}{v_\phi^2 + v^2 s_{2\beta}^2} f(m_{H^\pm}^2, m_A^2) \right. \\ &\quad \left. + \sum_{i=1}^3 R_{Si}^2 \left(\frac{v_\phi^2}{v_\phi^2 + v^2 s_{2\beta}^2} f(m_A^2, m_{h_i}^2) - f(m_{H^\pm}^2, m_{h_i}^2) \right) \right] \\ &\simeq \frac{1}{16\pi s_W^2 m_W^2} \left[m_{H^\pm}^2 - f(m_{H^\pm}^2, m_A^2) + \sum_{i=1}^3 R_{Si}^2 (f(m_A^2, m_{h_i}^2) - f(m_{H^\pm}^2, m_{h_i}^2)) \right], \end{aligned} \quad (4.6)$$

where R_{Si} is given in Appendix C, $f(x, y) \equiv xy \ln(x/y)/(x - y)$ and $f(x, x) = x$. As a result, a positive value of $\Delta\mathcal{T}$ can explain the W -boson mass excess. We calculate the W -boson mass excess as a function of m_{H^\pm} , fixing all other parameters and masses. For a given value of m_A and m_{h_2} , the excess, including the CDF-II measurement, can be justified within $m_{H^\pm}/m_A \gtrsim 1$ or in some regions for $m_{H^\pm}/m_A \lesssim 1$, except for $m_{H^\pm} = m_A$, m_{h_2} where $\Delta\mathcal{T} = 0$. Note that within the considered parameter space the h_3 contribution is negligible. In this case, the low-energy effective theory would be a 2HDM model that has the advantage of avoiding the strong CP problem thanks to the QCD axion. To relate the parameters of the DFSZ potential to those of a 2HDM, see Ref [76]. Also, in the whole studied problems, we also subtract the SM-like Higgs contribution in the calculation.

As we shall discuss in the following sections, the region of the parameter space that fits the lepton $g_l - 2$ anomalies corresponds to small values of κ , κ_d and κ_u , therefore, we fix $\kappa_d = \kappa_u = v^2/v_\phi^2$ and $\kappa = \tilde{\kappa} v^2/v_\phi$ with $\tilde{\kappa} < 1$.⁵ Furthermore, considering vacuum stability conditions (Appendix A), we impose perturbativity criteria as $\lambda, \lambda_{d,u} \lesssim 4\pi$. Therefore, in Fig. 1, we set other parameters as follows. Taking into account $m_{h_1} = 125$ GeV, we can find $\lambda_{d,u}$, fixing t_β and $\lambda_d - \lambda_u$. In this sense, since we obtain $\lambda_d - \lambda_u \approx \lambda_d$, we can fix $\lambda_d - \lambda_u < 4\pi$. In our calculations, we take $\lambda_d - \lambda_u = 5$. Within the considered parameter values, we can approximately express the mass terms of scalar fields, Eq. (2.9), with their first term for each relation.

Additionally, based on the perturbativity constraints from the Yukawa sector Eq. (2.4), we consider a conservative upper bound $t_\beta \leq 300$. According to the mass relation of the scalar fields, m_{h_3} , m_{h_2} , and m_A are also determined by fixing λ_ϕ , and then κ . Thus, we can plot m_W as a function of m_{H^\pm} . We consider m_{H^\pm} as a variable, although its different values can be obtained by fixing λ and $\tilde{\kappa}$. As shown in Fig. 1, we can obtain the W -boson mass excess within the parameter space of the theory, showing by three different benchmarks for $\kappa_d = \kappa_u = v^2/v_\phi^2$, $m_{h_1} = 125$ GeV, $\lambda_d - \lambda_u = 5$, $\lambda_\phi = 0.01$, $v_\phi = 10^9$ GeV and

⁵Such small values of couplings are also consistent with the notion of naturalness and enhancing the Poincaré symmetry [86].

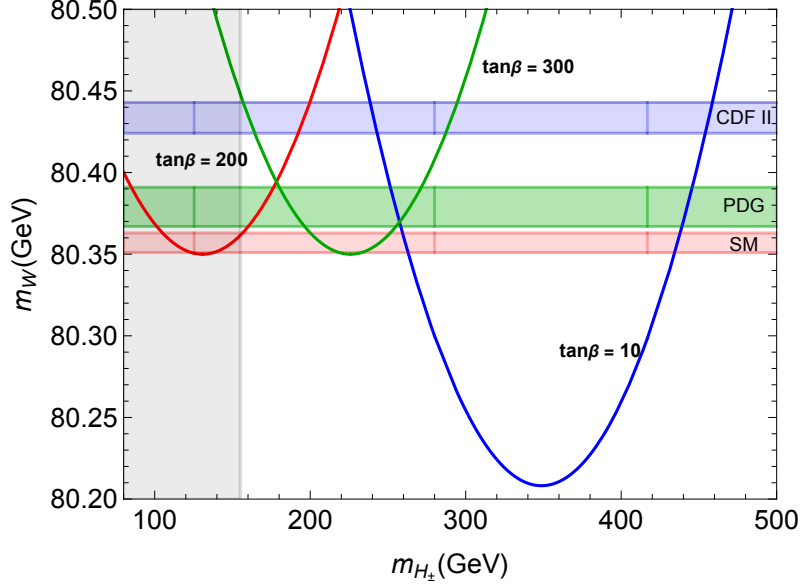


Figure 1. The W -boson mass m_W is shown as a function of m_{H^\pm} , for $\kappa_d = \kappa_u = v^2/v_\phi^2$, $m_{h_1} = 125$ GeV, $\lambda_d - \lambda_u = 5$, $\lambda_\phi = 0.01$, $v_\phi = 10^9$ GeV and three different values of $t_\beta = 10, 200, 300$ and $\tilde{\kappa} = 0.032, 0.00035, 0.001$ respectively. The relevant W -boson mass excess explanation with larger m_{H^\pm} can be found with larger $\tilde{\kappa}$.

three different values of $t_\beta = 10, 200, 300$ and $\tilde{\kappa} = 0.032, 0.00035, 0.0007$ respectively, which are corresponded to $\{m_A = 280$ GeV, $m_{h_2} = 417$ GeV, $m_{h_3} = 0.2v_\phi\}$, $\{m_A = 130$ GeV, $m_{h_2} = 131$ GeV, $m_{h_3} = 0.2v_\phi\}$, and $\{m_A = 226$ GeV, $m_{h_2} = 226$ GeV, $m_{h_3} = 0.2v_\phi\}$.

5 Lepton $g_l - 2$ anomalies

In this section, we first compute and discuss the analytical expressions for the lepton $g_l - 2$ anomalies, and then we proceed to calculate the magnetic moment of the muon and electron. On the basis of Lorentz covariance and gauge symmetry, the vertex of the QED interaction of a lepton can be expressed as

$$\bar{l}(p') \Gamma^\mu l(p) = \bar{l}(p') \left[\gamma^\mu F_1(q^2) + \frac{i \sigma^{\mu\nu} q_\nu F_2(q^2)}{2m_l} \right] l(p), \quad (5.1)$$

where $F_1(q^2)$ is related to the electric charge, and the lepton magnetic moment is defined as $a_l = F_2(0)$. Here, we calculate different Δa_l contributions from the model.

Regarding the Yukawa couplings, using a unitary transformation on the charged leptons, these Yukawa coupling matrices can be diagonalized, \tilde{y}_l , so that from Eqs. (2.4)

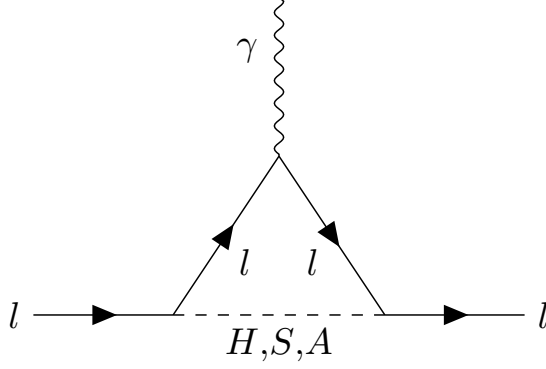


Figure 2. One-loop Feynman diagrams contributing to $g_l - 2$ from Higgs fields.

and (B.4), the Yukawa interactions of the leptonic sector, contributing to a_l , at one-loop level, can be expressed as

$$-\mathcal{L}_Y^l \supset -\frac{m_l}{v} \left(H \bar{l} l - t_\beta S \bar{l} l - i t_\beta \tilde{A} \bar{l} \gamma_5 l \right). \quad (5.2)$$

Therefore, from Eqs. (B.7) and (C.10) for mass eigenstates we obtain the one-loop amplitude, Fig. 2, as follows (checked by using **Package-X** [87])

$$\Delta a_l^{1L} = \frac{m_l^2}{16\pi^2 v^2} \left[\sum_{i=1}^3 (R_{H_i}^2 + t_\beta^2 R_{S_i}^2) F(x_{h_i}) + \frac{t_\beta^2 v_\phi^2}{v_\phi^2 + v^2 s_{2\beta}^2} F(x_A) \right], \quad (5.3)$$

where $x_{h_i} = m_l/m_{h_i}$, and $x_A = m_l/m_A$.⁶ The loop functions obtained, $F(x)$ and $F_{H\pm}(x, z)$ are given in Appendix D.

According to Eq. (2.4), the so-called Barr-Zee two-loop amplitudes can be obtained [89–91], where the dominant contribution, Fig. 3, is given by

$$\Delta a_l^{2L} = \sum_f \frac{\alpha m_l^2}{4\pi^3 v^2} N_C^f Q_f^2 \left[\sum_{i=1}^3 (R_{H_i}^2 \zeta_{f,l}^H + R_{S_i}^2 \zeta_{f,l}^{S,A}) \mathcal{F}(\omega_{h_i}) + \frac{\zeta_f^A v_\phi^2}{v_\phi^2 + v^2 s_{2\beta}^2} \tilde{\mathcal{F}}(\omega_A) \right], \quad (5.4)$$

where N_C^f is the number of colors and Q_f is the electric charge. Note that the two-loop contribution is at the α and \tilde{y}_l^2 level. We consider the dominant contribution from the t and b quarks, and therefore $\zeta_{t,l}^H = \zeta_{b,l}^H = 1$, $\zeta_{t,l}^{S,A} = -1$, $\zeta_{b,l}^{S,A} = t_\beta^2$. Also, $\omega_{h_i} = m_f^2/m_{h_i}^2$, $\omega_{h_i} = m_f^2/m_A^2$. The functions $\mathcal{F}(\omega)$ and $\tilde{\mathcal{F}}(\omega)$ are defined in Appendix D.

5.1 Muon $g_\mu - 2$ anomaly

Having obtained analytical formulas for $g_l - 2$, we investigate possible solutions to the anomalous magnetic moment of the muon and for the recently measured Δa_μ in Eq. (1.1). We show that the observed Δa_μ can be obtained for a range of t_β and small values of κ ,

⁶The contribution of the axion to Eq. (5.3) is proportional to $\frac{t_\beta^2 v^2 s_{2\beta}^2}{v_\phi^2 + v^2 s_{2\beta}^2} F(x_A)$ and is therefore negligible. For the contribution of EW gauge bosons, see, e.g. Ref. [88].

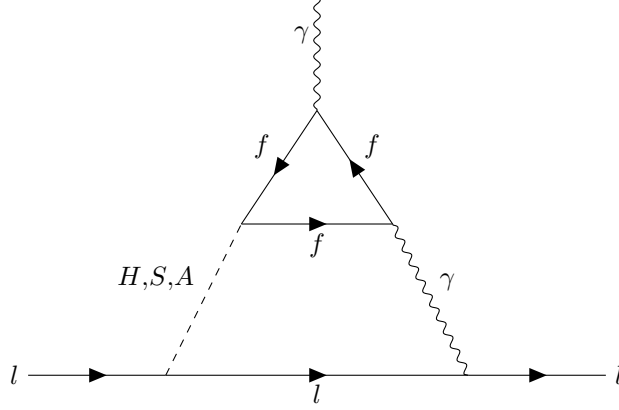


Figure 3. The Barr-Zee two-loop diagram contributing to $g_l - 2$.

κ_d , and κ_u , which is also consistent with the expansion of the scalar field mass spectra in terms of v/v_ϕ . In Fig. 4, we fix $\kappa_d = \kappa_u = v^2/v_\phi^2$, $m_{h_1} = 125$ GeV, $\lambda_\phi = 0.01$, $\lambda_d - \lambda_u = 5$, $v_\phi = 10^9$ GeV and obtain Δa_μ for a range of κ and some representative values of t_β that simultaneously determine the value of m_{h_3} , m_{h_2} and m_A , showing in terms of m_A .

As it can be seen in Fig. 4, we can find the observed anomaly for a range of t_β values. Taking into account the bounds from colliders on $m_A \gtrsim m_{h_1}/2$ [70], in addition to the small t_β , we can find the observed Δa_μ for $t_\beta \gtrsim 100$ ⁷. It should be noted that for $1 \lesssim t_\beta \lesssim 5$ the two-loop Barr-Zee contribution is dominated, whereas for other values of t_β the one- and two-loop contributions, which are at the same order in \tilde{y}_l , are almost equivalent. Additionally, in the small values of t_β , the top quark in the two-loop diagram contributes predominantly, while in the large values of t_β , the dominant contribution comes from the bottom quark. Furthermore, with $\lambda_d - \lambda_u \lesssim 0.2$, the result of interest is obtained only for large t_β .

5.2 Electron $g_e - 2$ anomaly

As already mentioned, due to the discrepancy in the measurement of α of Berkeley and LKB experiments, two different values have been reported for Δa_e , with opposite signs. Although results of the two experiments are rather inconsistent, we also study the averaged value case, combining the two results [94]

$$\Delta a_e^{\text{Avg}} = (-2 \pm 2.2) \times 10^{-13}. \quad (5.5)$$

We first try to explore possible explanations for Δa_e^{LBK} and Δa_e^{Avg} . We then study the physics which leads to the explanation of Δa_e^{B} , considering the constraints imposed by charged lepton flavor violation decays.

⁷In some type of 2HDMs, the anomalous muon magnetic moment can be explained for large t_β and a light pseudoscalar Higgs [92, 93].

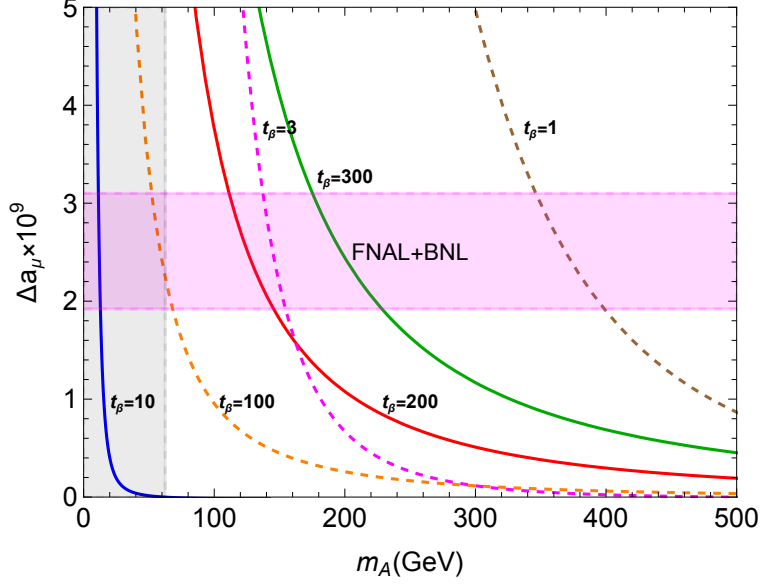


Figure 4. For $\kappa_d = \kappa_u = v^2/v_\phi^2$, $m_{h_1} = 125$ GeV, $\lambda_d - \lambda_u = 5$, $\lambda_\phi = 0.01$, $v_\phi = 10^9$ GeV, and different values of t_β , we show that the observed Δa_μ can be obtained, plotting as a function of m_A . The gray area shows the excluded region based on the bound $m_A \gtrsim m_{h_1}/2$ [70].

5.2.1 Δa_e^{LBK}

According to the LKB experiment and its result, Eq. (1.3), and because of the muon and electron mass difference, $m_e/m_\mu \sim 5 \times 10^{-3}$, it is expected to obtain positive Δa_e with the similar benchmark chosen for the case Δa_μ . Therefore, as shown in Fig. 5, we can find that Δa_e^{LBK} can be obtained as a function of m_A and t_β . It is shown that Δa_e^{LBK} can be explained for $1 \lesssim t_\beta \lesssim 3$ where the two-loop Barr-Zee contribution is dominated, while for large t_β , this is fulfilled for $t_\beta \gtrsim 500$. In these regions of the parameter space, based on our previous discussion, both the W -boson mass and Δa_μ anomalies can be explained. However, as can be seen from Figs. 5, 4, the range of m_A values explaining Δa_e^{LBK} and Δa_μ is different and thus both cannot be simultaneously explained.

As shown in Fig. 6, we also find that Δa_e^{Avg} can be obtained within the parameter space of the model. Interestingly, given the averaged value measured for the electron magnetic moment, in addition to the electron magnetic moment, the W -boson mass, and muon magnetic moment anomalies can be simultaneously explained for $t_\beta \gtrsim 120$. For instance with the following benchmark, for $\kappa_d = \kappa_u = v^2/v_\phi^2$, $m_{h_1} = 125$ GeV, $\lambda_d - \lambda_u = 5$, $\lambda_\phi = 0.01$, $v_\phi = 10^9$ GeV, $\lambda = 0.048$, $\tilde{\kappa} = 0.00035$ and $t_\beta = 200$, one can obtain $m_W \simeq 80.44$ GeV, $\Delta a_\mu \simeq 2.34 \times 10^{-9}$, and $\Delta a_e^{\text{Avg}} \simeq 0.17 \times 10^{-13}$. Also, as another example with the same parameters except for $\tan \beta = 300$ and $\tilde{\kappa} = 0.0007$, we find $m_W \simeq 80.43$ GeV, $\Delta a_\mu \simeq 2.08 \times 10^{-9}$, and $\Delta a_e^{\text{Avg}} \simeq 0.16 \times 10^{-13}$. These benchmark points are shown in

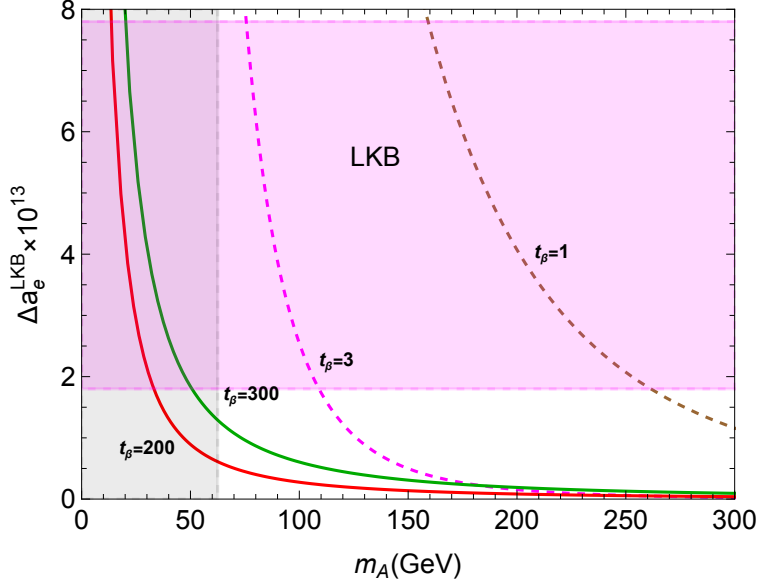


Figure 5. Similar to values chosen for parameters in the Fig. 4, for different values of t_β , we show that the observed Δa_e^{LKB} can be obtained with respect to m_A .

Figure 7 with red and green color, respectively.

5.2.2 Δa_e^{B}

As we discussed in the previous section, the parameter space of the model in which the W -boson mass and Δa_μ anomalies can be explained gives rise to a positive electron $g - 2$. Therefore, to explain the case of negative electron magnetic moment, Eq. (1.2), the mentioned model should be extended. Here we consider the model supplemented with heavy RH neutrinos, which are PQ charged and SM singlet, and study their contribution to the lepton $g_l - 2$.

The Lagrangian for right-handed neutrinos is given by

$$\mathcal{L}_N = \bar{N}_{R_\alpha} i \partial_\mu N_{R_\alpha} - m_{N_{R_\alpha}} \bar{N}_{R_\alpha} N_{R_\alpha}^c - y_{N_\alpha}^l \bar{\Psi}_{L_l} \tilde{H}_d N_{R_\alpha} + \text{H.c.}, \quad (5.6)$$

where N_{R_α} are RH neutrinos. Then, the Yukawa interaction of the charged Higgs and RH neutrinos can be expressed as⁸

$$\sqrt{2} t_\beta y_{N_\alpha}^l H_+ \bar{l} P_R N_\alpha + \text{H.c.}. \quad (5.7)$$

Therefore, according to the relevant Feynman diagram, Fig. 8, an additional one-loop

⁸Here, we do not discuss the mechanism describing light neutrino masses and consider $y_{N_\alpha}^l$ as a variable with its diagonal form.

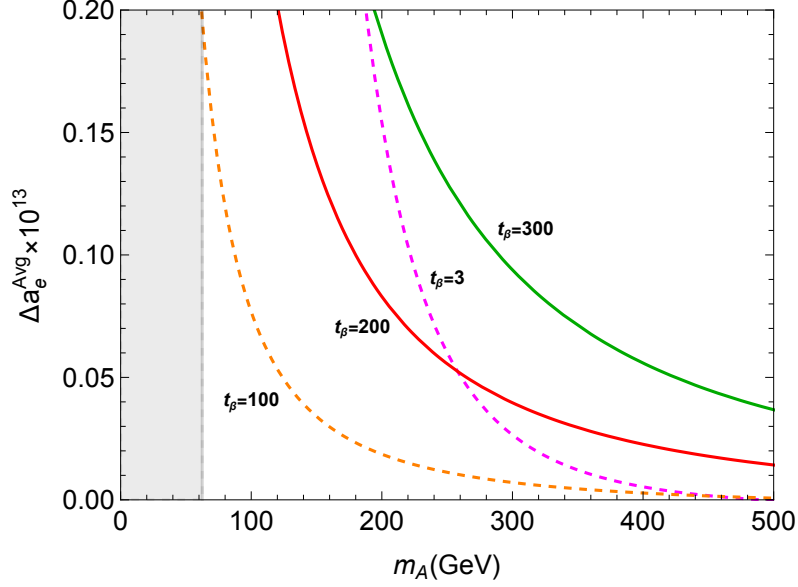


Figure 6. Similar to values chosen for parameters in the Fig. 4, for different values of t_β , we show that Δa_e^{Avg} can be obtained, plotting as a function of m_A . The whole range of Δa_e^{Avg} axis in this plot is allowed based on the average experimental bound. Because of the obtained positive results, negative values of Eq. (5.5) in the Δa_e^{Avg} axis are not shown.

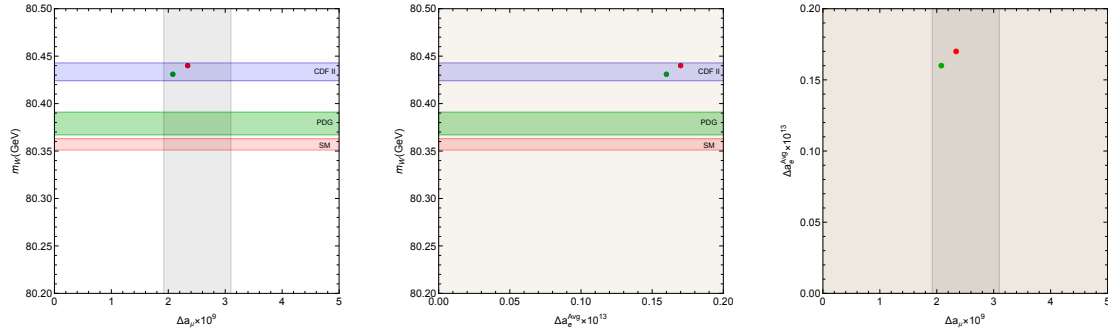


Figure 7. Benchmark points, associated with $t_\beta = 200$ (red) and $t_\beta = 300$ (green), are represented, satisfying different experimental bounds for M_W , Δa_μ and Δa_e^{Avg} discussed in previous sections. Also, different experimental constraints are shown in three panels.

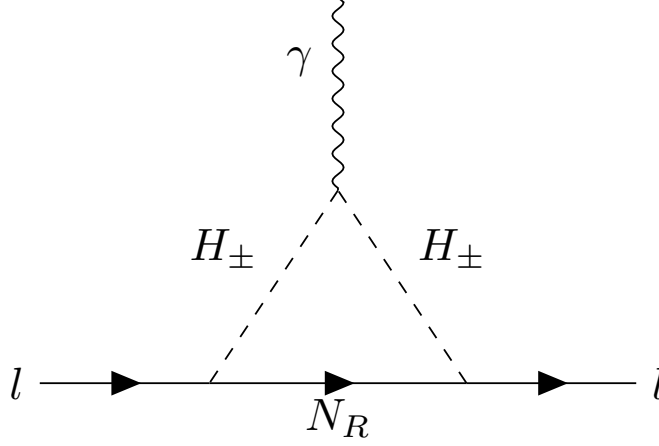


Figure 8. One-loop Feynman diagrams contributing to $(g_l - 2)$ from charged Higgs fields and heavy neutrinos.

amplitude should be calculated and (checked by using **Package-X** [87]) the result would be as follows

$$\Delta a_l^{1L} = \sum_{\alpha=1}^{n_R} \frac{t_\beta^2 (y_{N_\alpha}^l)^2}{8\pi^2} F_{H^\pm}(x_{H^\pm}, z_{H^\pm}), \quad (5.8)$$

where $x_{H^\pm} = m_l/m_{H^\pm}$, $z_{H^\pm} = m_{N_{R\alpha}}/m_{H^\pm}$, and n_R is the number of RH neutrinos. In our calculations, we assume $n_R = 3$ and the same properties for all generations.

Since this additional contribution, Eq. (5.8), is negative, its effect on the muon magnetic moment should also be noted. For very heavy RH neutrinos, the contribution of this term is negligible. However, as shown in Fig. 9, for $y_N^\mu \gtrsim 0.01$ and sufficiently light RH neutrinos, Δa_μ can be negative, and hence we consider it $y_N^\mu < 0.01$ in the calculations.

Before proceeding to calculate the electron magnetic moment for this case, we first discuss another constraint. Charged lepton flavor violations are highly constrained and the bound on the branching ratio of the decay $\mu \rightarrow e\gamma$ is more severe [95]

$$\text{Br}(\mu \rightarrow e\gamma) < 4.2 \times 10^{-13}. \quad (5.9)$$

Thus, we can constrain the model as follows

$$\text{Br}(\mu \rightarrow e\gamma) \sim \frac{96\pi^3 \alpha v^4}{m_\mu^4} a_{\mu e}^2, \quad (5.10)$$

where

$$a_{\mu e} = \sum_{\alpha=1}^{n_R} \frac{t_\beta^2 y_{N_\alpha}^\mu y_{N_\alpha}^e}{8\pi^2} \mathcal{F}_{H^\pm}, \quad (5.11)$$

and the function obtained \mathcal{F}_{H^\pm} is given in Appendix D.⁹ According to Eq. (5.9), we should have $|a_{\mu e}| < 2.5 \times 10^{-14}$. To pass the flavor violation decay bound, based on the previous

⁹Note that for this constraint, we consider the case where the coupling of RH neutrinos and muon (muon neutrino), $y_{N_\alpha}^\mu$, is non-zero.

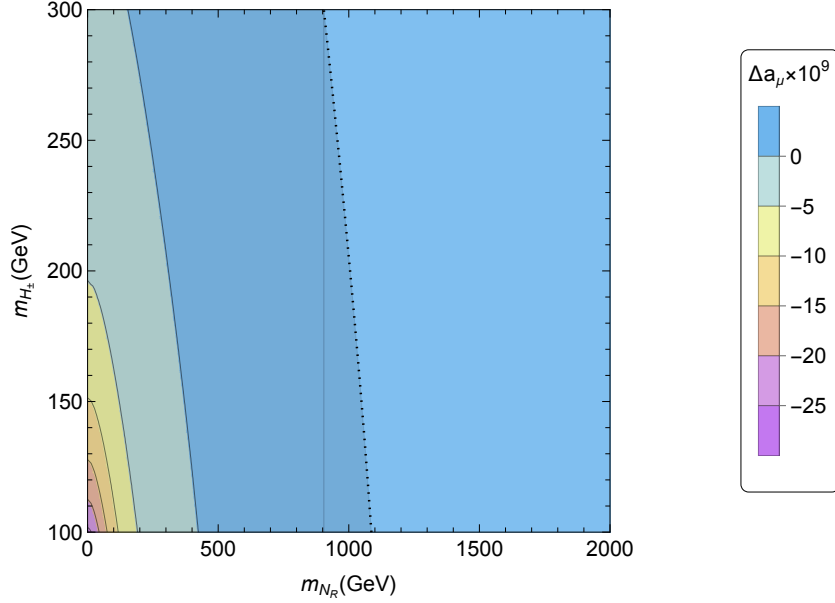


Figure 9. For $\kappa_d = \kappa_u = v^2/v_\phi^2$, $m_{h_1} = 125$ GeV, $\lambda_\phi = 0.01$, $\lambda_d - \lambda_u = 5$, $v_\phi = 10^9$ GeV, $t_\beta = 200$, $m_A = 130$ GeV and $y_N^\mu = 0.01$, we find Δa_μ as a function of m_{N_R} and m_{H^\pm} . The colored regions show different values of the muon magnetic moment which could be even negative for small values of m_{N_R} with $y_N^\mu = 0.01$. For $y_N^\mu < 0.01$ the negative contribution, Eq. (5.8), to Δa_μ would be negligible. The region on the left of dashed grey line is excluded by the PDG $(g-2)_\mu$ bound.

estimation on $y_N^\mu < 0.01$, with calculating $a_{\mu e}$, the hierarchy $y_N^\mu \ll y_N^e$ can be imposed, taking $y_N^e < 4\pi$. For example, in Fig. 10, we show that $|a_{\mu e}| < 2.5 \times 10^{-14}$ can be obtained for $y_N^e \leq 0.2$ and $y_N^\mu = 10^{-7}$. Considering such bounds on the parameters, we obtain the electron magnetic moment and if Δa_e^B is the case, we find that taking $y_N^e < 4\pi$, the measured quantity can be obtained for $m_{N_R} \lesssim 200$ TeV. In Fig. 11, we show the result for $y_N^e \leq 0.2$.

6 Conclusion

Recent measurements of the muon magnetic moment, the W -boson mass, and their deviation from the SM prediction can imply new physics beyond the SM. In this paper, in light of these observations we have studied a QCD axion model, enjoying the PQ symmetry, as an attractive framework that can address other SM shortcomings including the strong CP and the DM problem.

We considered the DFSZ axion model and calculated loop-level diagrams that contribute to the muon and the electron magnetic moment, and W -boson mass. Considering the lower bound on the mass of charged Higgs, we have shown that the CDF-II W boson mass excess can be addressed within the parameter space of the model, except for the case $m_{H^\pm} = m_A, m_{h_2}$. We have also shown that the positive muon magnetic moment Δa_μ can

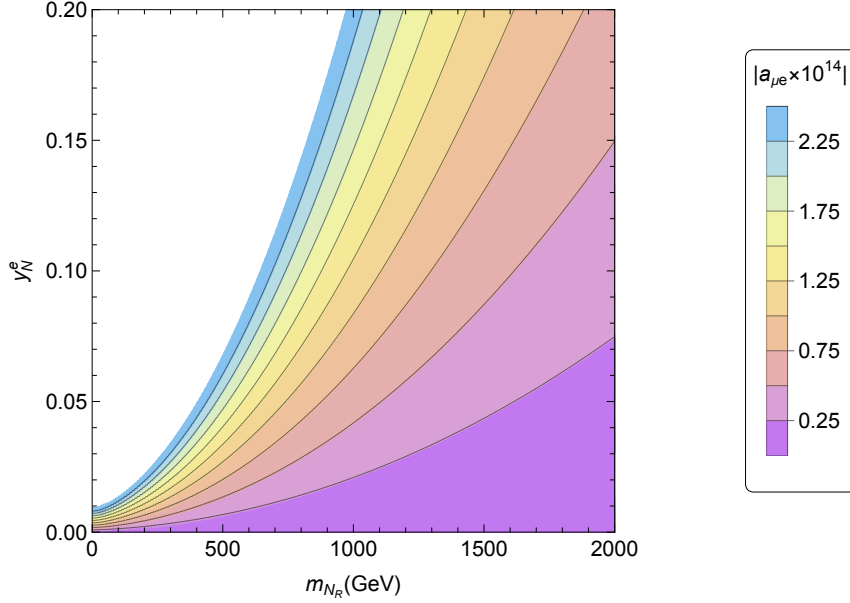


Figure 10. For $\kappa_d = \kappa_u = v^2/v_\phi^2$, $m_{h_1} = 125$ GeV, $\lambda_\phi = 0.01$, $\lambda_d - \lambda_u = 5$, $v_\phi = 10^9$ GeV, $t_\beta = 200$, $m_A = 130$ GeV, $m_{H^\pm} = 160$ GeV, and $y_N^\mu = 10^{-7}$, we show that $|a_{\mu e}| < 2.5 \times 10^{-14}$ can be obtained, plotting as a function of m_{N_R} and y_N^e . All colored regions are consistent with the bound.

be obtained for a range of t_β values with a mass range of extra Higgs bosons at the EW scale, respecting the direct collider bound on the pseudoscalar field and also theoretical constraints.

Regarding the electron $g-2$, there are Berkeley and LKB experiments whose measurements are set in opposite directions. We showed that Δa_e^{LBK} can be explained within a different region of the parameter space allowed for Δa_μ . However, we found that considering the averaged value of the two experiments, the three anomalies can be simultaneously explained. The electron magnetic moment measured by another experiment at Berkeley, Δa_e^{B} , is of a different sign and the physics that explains Δa_μ and the W -boson mass excess leads to a positive electron $g-2$. To address Δa_μ , Δa_e^{B} , and the W -boson mass anomalies simultaneously, we extended the model with heavy RH neutrinos. Taking into account the flavor violation decay bounds, we found that heavy neutrino-charged Higgs interactions contributing to one-loop diagrams that can be responsible for the negative Δa_e with heavy neutrinos masses up to 200 TeV.

Acknowledgments

The authors would like to thank Nicloás Bernal for insightful discussions and comments. Also, they are grateful to Heinrich Päs for reading the early version of our manuscript. FH is supported by the research grant “New Theoretical Tools for Axion Cosmology”

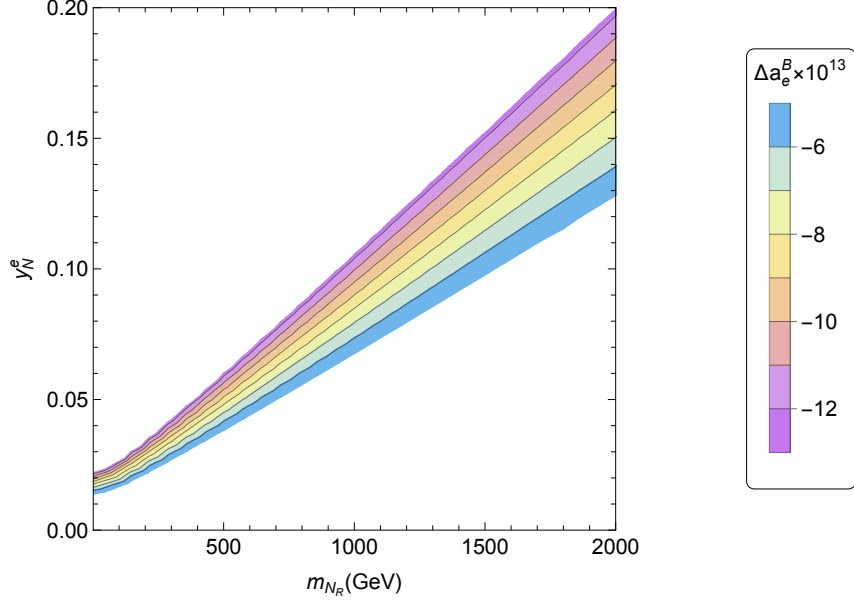


Figure 11. For $\kappa_d = \kappa_u = v^2/v_\phi^2$, $m_{h_1} = 125$ GeV, $\lambda_\phi = 0.01$, $\lambda_d - \lambda_u = 5$, $v_\phi = 10^9$ GeV, $t_\beta = 200$, $m_A = 130$ GeV, and $m_{H^\pm} = 160$ GeV, Δa_e^B as a function of m_{N_R} and y_N^e is shown. The colored regions show different negative values of the electron magnetic moment.

under the Supporting TAlent in ReSeArch@University of Padova (STARS@UNIPD), Istituto Nazionale di Fisica Nucleare (INFN) through the Theoretical Astroparticle Physics (TAsP) project. FH also thanks the organizers of the “Probing New Physics with Gravitational Waves” Workshop 2022 at the Mainz Institute for Theoretical Physics (MITP) of the Cluster of Excellence PRISMA (Project ID 39083149) in Mainz, for hospitality and partial financial support during the completion of this work.

A Minimization and vacuum stability conditions

We can use the minimization of the potential, Eq. (2.3), and remove three parameters μ_d , μ_u and V_ϕ , expressing in terms of free parameters as follows

$$2\lambda_d v^2 c_\beta^2 - \mu_d^2 + \frac{v_\phi^2}{2} \left(\kappa_d - \frac{\kappa \tan \beta}{v_\phi} \right) = 0, \quad (\text{A.1})$$

$$2\lambda_u v^2 s_\beta^2 - \mu_u^2 + \frac{v_\phi^2}{2} \left(\kappa_u - \frac{\kappa}{v_\phi \tan \beta} \right) = 0, \quad (\text{A.2})$$

$$\lambda_\phi (v_\phi^2 - V_\phi^2) + 2v^2 \left(\kappa_d c_\beta^2 + \kappa_u s_\beta^2 - \frac{\kappa s_{2\beta}}{v_\phi} \right) = 0. \quad (\text{A.3})$$

Assuming that κ_d , κ_u and κ are sufficiently small and do not affect the vacuum stability conditions obtained from other quartic terms of the potential, we have

$$\begin{aligned}\lambda_\phi &> 0, \quad \lambda_d > 0, \quad \lambda_u > 0, \\ \lambda + 2\sqrt{\lambda_d \lambda_u} &> 0.\end{aligned}\tag{A.4}$$

B Rotations for the Higgs fields

With the following rotated Higgs doublets, one can find the direction by which unphysical components are removed

$$H'_d = c_\beta H_d + s_\beta H_u = \frac{1}{\sqrt{2}} \begin{pmatrix} c_\beta \alpha^+ + s_\beta \beta^+ \\ c_\beta \text{Re}[\alpha_0] + s_\beta \text{Re}[\beta_0] + i(c_\beta \text{Im}[\alpha_0] + s_\beta \text{Im}[\beta_0]) \end{pmatrix}, \tag{B.1}$$

where $c_\beta \equiv \cos \beta$ and $s_\beta \equiv \sin \beta$. The upper components are combinations absorbed by W^\pm and the real part is the component with non-zero vev, thus H'_d has the structure of SM doublet so that

$$\langle c_\beta \text{Re}[\alpha_0] + s_\beta \text{Re}[\beta_0] \rangle = c_\beta v_d + s_\beta v_u = v \tag{B.2}$$

and $\langle H + v \rangle = v$. Also, the other rotated doublet would be

$$H'_u = -s_\beta H_d + c_\beta H_u = \frac{1}{\sqrt{2}} \begin{pmatrix} -s_\beta \alpha^+ + c_\beta \beta^+ \\ -s_\beta \text{Re}[\alpha_0] + c_\beta \text{Re}[\beta_0] + i(-s_\beta \text{Im}[\alpha_0] + c_\beta \text{Im}[\beta_0]) \end{pmatrix}, \tag{B.3}$$

whose charged components denote the charged Higgs H^\pm and the real neutral component is a scalar Higgs S such that $\langle S \rangle = \langle -s_\beta \text{Re}[\alpha_0] + c_\beta \text{Re}[\beta_0] \rangle = 0$. Therefore, the gauge-redefined doublets can be expressed as

$$H_d = c_\beta H'_d - s_\beta H'_u = \frac{1}{\sqrt{2}} \begin{pmatrix} -\sqrt{2}s_\beta H^+ \\ (v + H) c_\beta - s_\beta (S + i\tilde{A}) \end{pmatrix}, \tag{B.4}$$

$$H_u = s_\beta H'_d + c_\beta H'_u = \frac{1}{\sqrt{2}} \begin{pmatrix} \sqrt{2}c_\beta H^+ \\ (v + H) s_\beta + c_\beta (S + i\tilde{A}) \end{pmatrix}. \tag{B.5}$$

Although \tilde{A} remains after gauge redefinition, the field is not yet physical. Moreover, from $\phi = v_\phi + \varrho + i\tilde{G}$, \tilde{G} is another non-physical d.o.f. whose combination with \tilde{A} identifies the physical one in the pseudoscalar sector [76]. In addition to the massless eigenstate, the axion resulting from the PQ current is

$$a = \frac{v_\phi \tilde{G} + v s_{2\beta} \tilde{A}}{\sqrt{v_\phi^2 + v^2 s_{2\beta}^2}}. \tag{B.6}$$

There is also a massive pseudoscalar eigenstate, evident from the cubic term in the potential, as

$$A = \frac{v_\phi \tilde{A} - v s_{2\beta} \tilde{G}}{\sqrt{v_\phi^2 + v^2 s_{2\beta}^2}}. \tag{B.7}$$

C The mass matrix of neutral scalar fields

The mass matrix of the neutral CP-even scalar fields is given by

$$M = \begin{pmatrix} 32v^2 (\lambda_d c_\beta^4 + \lambda_u s_\beta^4) & M_{12} & M_{13} \\ M_{21} & \frac{8\kappa v_\phi}{s_{2\beta}} + 8v^2 (\lambda_d + \lambda_u) s_{2\beta}^2 & M_{23} \\ M_{31} & M_{32} & 4\lambda_\phi v_\phi^2 \end{pmatrix}, \quad (\text{C.1})$$

where

$$M_{12} = M_{21} = 16v^2 (-\lambda_d c_\beta^2 + \lambda_u s_\beta^2) s_{2\beta}, \quad (\text{C.2})$$

$$M_{13} = M_{31} = 8vv_\phi (\kappa_d c_\beta^2 + \kappa_u s_\beta^2 - \kappa s_{2\beta}/v_\phi), \quad (\text{C.3})$$

$$M_{23} = M_{32} = -4vv_\phi [(\kappa_d - \kappa_u) s_{2\beta} + 2\kappa c_{2\beta}/v_\phi]. \quad (\text{C.4})$$

The rotation matrix can be written as [76]

$$R = \exp \left(\frac{v}{v_\phi} \mathcal{A} + \frac{v^2}{v_\phi^2} \mathcal{B} \right), \quad \mathcal{A}^T = -\mathcal{A}, \quad \mathcal{B}^T = -\mathcal{B}, \quad (\text{C.5})$$

so that

$$R = \begin{pmatrix} 1 - \frac{v^2}{v_\phi^2} \frac{\mathcal{A}_{13}^2}{2} & \frac{v^2}{v_\phi^2} \frac{\mathcal{A}_{13}\mathcal{A}_{23} + 2\mathcal{B}_{12}}{2} & \frac{v}{v_\phi} \mathcal{A}_{13} \\ -\frac{v^2}{v_\phi^2} \frac{\mathcal{A}_{13}\mathcal{A}_{23} + 2\mathcal{B}_{12}}{2} & 1 - \frac{v^2}{v_\phi^2} \frac{\mathcal{A}_{23}^2}{2} & \frac{v}{v_\phi} \mathcal{A}_{23} \\ -\frac{v}{v_\phi} \mathcal{A}_{13} & -\frac{v}{v_\phi} \mathcal{A}_{23} & 1 - \frac{v^2}{v_\phi^2} \frac{\mathcal{A}_{13}^2 + \mathcal{A}_{23}^2}{2} \end{pmatrix}, \quad (\text{C.6})$$

where

$$\mathcal{A}_{13} = \frac{2}{\lambda_\phi} (\kappa_d c_\beta^2 + \kappa_u s_\beta^2 - \kappa s_{2\beta}/v_\phi), \quad \mathcal{A}_{23} = \frac{(\kappa_d - \kappa_u) s_{2\beta} + 2\kappa c_{2\beta}/v_\phi}{\frac{2\kappa}{v_\phi s_{2\beta}} - \lambda_\phi}, \quad (\text{C.7})$$

$$\begin{aligned} \mathcal{B}_{12} = & -\frac{2v_\phi}{\kappa} s_{2\beta}^2 (\lambda_d c_\beta^2 - \lambda_u s_\beta^2) \\ & + \frac{v_\phi s_{2\beta}}{\lambda_\phi \kappa} \frac{\kappa - v_\phi \lambda_\phi s_{2\beta}}{2\kappa - v_\phi \lambda_\phi s_{2\beta}} \left(\kappa_d c_\beta^2 + \kappa_u s_\beta^2 - \frac{\kappa s_{2\beta}}{v_\phi} \right) \left[(\kappa_d - \kappa_u) s_{2\beta} + \frac{2\kappa c_{2\beta}}{v_\phi} \right], \end{aligned} \quad (\text{C.8})$$

and up to second order in v/v_ϕ , $\mathcal{A}_{12} = \mathcal{B}_{13} = \mathcal{B}_{23} = 0$. Thus, the scalar states are related to the mass eigenstates h_i , as

$$\begin{pmatrix} H \\ S \\ \varrho \end{pmatrix} = R \begin{pmatrix} h_1 \\ h_2 \\ h_3 \end{pmatrix}. \quad (\text{C.9})$$

so that

$$H = \sum_{i=1}^3 R_{Hi} h_i, \quad S = \sum_{i=1}^3 R_{Si} h_i, \quad \varrho = \sum_{i=1}^3 R_{\varrho i} h_i. \quad (\text{C.10})$$

D Loop functions

Loop functions of one-loop calculations used in Section 5 are given as follows

$$F(x) = \frac{(3x^2 - 2)x^2 + (3x^2 - 1)\ln(x^2) + 2(x^2 - 1)\sqrt{1 - 4x^2}\ln\left(\frac{1 + \sqrt{1 - 4x^2}}{2x}\right)}{x^4}, \quad (\text{D.1})$$

$$F_{H^\pm}(x, z) = \frac{x^2 + 2z^2 - 2}{2x^2} + \frac{(x^2 - (z^2 - 1)^2)\log(z^2)}{2x^4} - \frac{\left(x^4 + x^2(z^4 + z^2 - 2) - (z^2 - 1)^3\right)\log\left(\frac{(-x^2 + z^2 + 1) + \sqrt{-2(x^2 + 1)z^2 + (x^2 - 1)^2 + z^4}}{2z}\right)}{x^4\sqrt{x^4 - 2x^2(z^2 + 1) + (z^2 - 1)^2}}, \quad (\text{D.2})$$

and functions of the two-loop amplitude can be computed by

$$\mathcal{F}(\omega) = \frac{\omega}{2} \int_0^1 dx \frac{2x(1-x) - 1}{x(1-x) - \omega} \log \frac{x(1-x)}{\omega}, \quad (\text{D.3})$$

$$\tilde{\mathcal{F}}(\omega) = \frac{\omega}{2} \int_0^1 dx \frac{1}{x(1-x) - \omega} \log \frac{x(1-x)}{\omega}. \quad (\text{D.4})$$

Moreover, the function associated with the calculation of the lepton flavor violation process is obtained as

$$\begin{aligned} \mathcal{F}_{H^\pm} = & \frac{(m_\mu m_e^2 - m_\mu m_{H^\pm}^2 + m_\mu m_N^2 - 2m_e m_{H^\pm}^2 + 2m_e m_N^2) \Lambda(m_e^2, m_{H^\pm}, m_N)}{4m_e(m_\mu^2 - m_e^2)} \\ & - \frac{(m_\mu^2 m_e - 2m_\mu m_{H^\pm}^2 + 2m_\mu m_N^2 - m_e m_{H^\pm}^2 + m_e m_N^2) \Lambda(m_\mu^2, m_{H^\pm}, m_N)}{4m_\mu(m_\mu^2 - m_e^2)} \\ & + \frac{1}{2} m_{H^\pm}^2 C_0(0, m_\mu^2, m_e^2, m_{H^\pm}, m_{H^\pm}, m_N) + \frac{m_\mu m_e - m_{H^\pm}^2 + m_N^2}{4m_\mu m_e} \\ & - \frac{\log\left(\frac{m_{H^\pm}^2}{m_N^2}\right) (2m_\mu^2 m_e^2 m_{H^\pm}^2 - m_\mu^2 m_{H^\pm}^4 + 2m_\mu^2 m_{H^\pm}^2 m_N^2 - m_\mu^2 m_N^4 - 2m_\mu m_e m_{H^\pm}^4)}{8m_\mu^3 m_e^3} \\ & - \frac{\log\left(\frac{m_{H^\pm}^2}{m_N^2}\right) (4m_\mu m_e m_{H^\pm}^2 m_N^2 - 2m_\mu m_e m_N^4 - m_e^2 m_{H^\pm}^4 + 2m_e^2 m_{H^\pm}^2 m_N^2 - m_e^2 m_N^4)}{8m_\mu^3 m_e^3}, \end{aligned} \quad (\text{D.5})$$

where Λ (`DiscB`) and C_0 (`ScalarC0`) are Veltmann-Passarino functions that are also defined in the `Package-X` program.

References

- [1] R.D. Peccei and H.R. Quinn, *CP Conservation in the Presence of Instantons*, *Phys. Rev. Lett.* **38** (1977) 1440.
- [2] R.D. Peccei and H.R. Quinn, *Some Aspects of Instantons*, *Nuovo Cim. A* **41** (1977) 309.

- [3] R.D. Peccei, *The Strong CP problem and axions*, *Lect. Notes Phys.* **741** (2008) 3 [[hep-ph/0607268](#)].
- [4] S. Weinberg, *A New Light Boson?*, *Phys. Rev. Lett.* **40** (1978) 223.
- [5] F. Wilczek, *Problem of Strong P and T Invariance in the Presence of Instantons*, *Phys. Rev. Lett.* **40** (1978) 279.
- [6] J. Preskill, M.B. Wise and F. Wilczek, *Cosmology of the Invisible Axion*, *Phys. Lett. B* **120** (1983) 127.
- [7] L.F. Abbott and P. Sikivie, *A Cosmological Bound on the Invisible Axion*, *Phys. Lett. B* **120** (1983) 133.
- [8] M. Dine and W. Fischler, *The Not So Harmless Axion*, *Phys. Lett. B* **120** (1983) 137.
- [9] R.L. Davis, *Goldstone Bosons in String Models of Galaxy Formation*, *Phys. Rev. D* **32** (1985) 3172.
- [10] D.J.E. Marsh, *Axion Cosmology*, *Phys. Rept.* **643** (2016) 1 [[1510.07633](#)].
- [11] L. Di Luzio, M. Giannotti, E. Nardi and L. Visinelli, *The landscape of QCD axion models*, *Phys. Rept.* **870** (2020) 1 [[2003.01100](#)].
- [12] MUON G-2 collaboration, *Measurement of the Positive Muon Anomalous Magnetic Moment to 0.46 ppm*, *Phys. Rev. Lett.* **126** (2021) 141801 [[2104.03281](#)].
- [13] MUON G-2 collaboration, *Final Report of the Muon E821 Anomalous Magnetic Moment Measurement at BNL*, *Phys. Rev. D* **73** (2006) 072003 [[hep-ex/0602035](#)].
- [14] T. Aoyama et al., *The anomalous magnetic moment of the muon in the Standard Model*, *Phys. Rept.* **887** (2020) 1 [[2006.04822](#)].
- [15] T. Aoyama, M. Hayakawa, T. Kinoshita and M. Nio, *Complete Tenth-Order QED Contribution to the Muon g-2*, *Phys. Rev. Lett.* **109** (2012) 111808 [[1205.5370](#)].
- [16] T. Aoyama, T. Kinoshita and M. Nio, *Theory of the Anomalous Magnetic Moment of the Electron*, *Atoms* **7** (2019) 28.
- [17] A. Czarnecki, W.J. Marciano and A. Vainshtein, *Refinements in electroweak contributions to the muon anomalous magnetic moment*, *Phys. Rev. D* **67** (2003) 073006 [[hep-ph/0212229](#)].
- [18] C. Gnendiger, D. Stöckinger and H. Stöckinger-Kim, *The electroweak contributions to $(g-2)_\mu$ after the Higgs boson mass measurement*, *Phys. Rev. D* **88** (2013) 053005 [[1306.5546](#)].
- [19] M. Davier, A. Hoecker, B. Malaescu and Z. Zhang, *Reevaluation of the hadronic vacuum polarisation contributions to the Standard Model predictions of the muon $g-2$ and $\alpha(m_Z^2)$ using newest hadronic cross-section data*, *Eur. Phys. J. C* **77** (2017) 827 [[1706.09436](#)].
- [20] A. Keshavarzi, D. Nomura and T. Teubner, *Muon $g-2$ and $\alpha(M_Z^2)$: a new data-based analysis*, *Phys. Rev. D* **97** (2018) 114025 [[1802.02995](#)].
- [21] G. Colangelo, M. Hoferichter and P. Stoffer, *Two-pion contribution to hadronic vacuum polarization*, *JHEP* **02** (2019) 006 [[1810.00007](#)].
- [22] M. Hoferichter, B.-L. Hoid and B. Kubis, *Three-pion contribution to hadronic vacuum polarization*, *JHEP* **08** (2019) 137 [[1907.01556](#)].

- [23] M. Davier, A. Hoecker, B. Malaescu and Z. Zhang, *A new evaluation of the hadronic vacuum polarisation contributions to the muon anomalous magnetic moment and to $\alpha(m_Z^2)$* , *Eur. Phys. J. C* **80** (2020) 241 [[1908.00921](#)].
- [24] A. Keshavarzi, D. Nomura and T. Teubner, *$g - 2$ of charged leptons, $\alpha(M_Z^2)$, and the hyperfine splitting of muonium*, *Phys. Rev. D* **101** (2020) 014029 [[1911.00367](#)].
- [25] A. Kurz, T. Liu, P. Marquard and M. Steinhauser, *Hadronic contribution to the muon anomalous magnetic moment to next-to-next-to-leading order*, *Phys. Lett. B* **734** (2014) 144 [[1403.6400](#)].
- [26] K. Melnikov and A. Vainshtein, *Hadronic light-by-light scattering contribution to the muon anomalous magnetic moment revisited*, *Phys. Rev. D* **70** (2004) 113006 [[hep-ph/0312226](#)].
- [27] P. Masjuan and P. Sanchez-Puertas, *Pseudoscalar-pole contribution to the $(g_\mu - 2)$: a rational approach*, *Phys. Rev. D* **95** (2017) 054026 [[1701.05829](#)].
- [28] G. Colangelo, M. Hoferichter, M. Procura and P. Stoffer, *Dispersion relation for hadronic light-by-light scattering: two-pion contributions*, *JHEP* **04** (2017) 161 [[1702.07347](#)].
- [29] M. Hoferichter, B.-L. Hoid, B. Kubis, S. Leupold and S.P. Schneider, *Dispersion relation for hadronic light-by-light scattering: pion pole*, *JHEP* **10** (2018) 141 [[1808.04823](#)].
- [30] A. Gérardin, H.B. Meyer and A. Nyffeler, *Lattice calculation of the pion transition form factor with $N_f = 2 + 1$ Wilson quarks*, *Phys. Rev. D* **100** (2019) 034520 [[1903.09471](#)].
- [31] J. Bijnens, N. Hermansson-Truedsson and A. Rodríguez-Sánchez, *Short-distance constraints for the $HLbL$ contribution to the muon anomalous magnetic moment*, *Phys. Lett. B* **798** (2019) 134994 [[1908.03331](#)].
- [32] G. Colangelo, F. Hagelstein, M. Hoferichter, L. Laub and P. Stoffer, *Longitudinal short-distance constraints for the hadronic light-by-light contribution to $(g - 2)_\mu$ with large- N_c Regge models*, *JHEP* **03** (2020) 101 [[1910.13432](#)].
- [33] T. Blum, N. Christ, M. Hayakawa, T. Izubuchi, L. Jin, C. Jung et al., *Hadronic Light-by-Light Scattering Contribution to the Muon Anomalous Magnetic Moment from Lattice QCD*, *Phys. Rev. Lett.* **124** (2020) 132002 [[1911.08123](#)].
- [34] G. Colangelo, M. Hoferichter, A. Nyffeler, M. Passera and P. Stoffer, *Remarks on higher-order hadronic corrections to the muon $g - 2$* , *Phys. Lett. B* **735** (2014) 90 [[1403.7512](#)].
- [35] R.H. Parker, C. Yu, W. Zhong, B. Estey and H. Müller, *Measurement of the fine-structure constant as a test of the Standard Model*, *Science* **360** (2018) 191 [[1812.04130](#)].
- [36] D. Hanneke, S. Fogwell and G. Gabrielse, *New Measurement of the Electron Magnetic Moment and the Fine Structure Constant*, *Phys. Rev. Lett.* **100** (2008) 120801 [[0801.1134](#)].
- [37] D. Hanneke, S.F. Hoogerheide and G. Gabrielse, *Cavity Control of a Single-Electron Quantum Cyclotron: Measuring the Electron Magnetic Moment*, *Phys. Rev. A* **83** (2011) 052122 [[1009.4831](#)].
- [38] L. Morel, Z. Yao, P. Cladé and S. Guellati-Khélifa, *Determination of the fine-structure constant with an accuracy of 81 parts per trillion*, *Nature* **588** (2020) 61.
- [39] CDF collaboration, *High-precision measurement of the W boson mass with the CDF II detector*, *Science* **376** (2022) 170.
- [40] PARTICLE DATA GROUP collaboration, *Review of Particle Physics*, *PTEP* **2022** (2022) 083C01.

- [41] P. Athron, A. Fowlie, C.-T. Lu, L. Wu, Y. Wu and B. Zhu, *The W boson Mass and Muon $g - 2$: Hadronic Uncertainties or New Physics?*, [2204.03996](#).
- [42] O. Popov and G.A. White, *One Leptoquark to unify them? Neutrino masses and unification in the light of $(g - 2)_\mu$, $R_{D^{(*)}}$ and R_K anomalies*, *Nucl. Phys. B* **923** (2017) 324 [[1611.04566](#)].
- [43] L. Delle Rose, S. Khalil and S. Moretti, *Explaining electron and muon $g - 2$ anomalies in an Aligned 2-Higgs Doublet Model with right-handed neutrinos*, *Phys. Lett. B* **816** (2021) 136216 [[2012.06911](#)].
- [44] G. Cacciapaglia and F. Sannino, *The W boson mass weighs in on the non-standard Higgs*, *Phys. Lett. B* **832** (2022) 137232 [[2204.04514](#)].
- [45] H.M. Lee and K. Yamashita, *A model of vector-like leptons for the muon $g - 2$ and the W boson mass*, *Eur. Phys. J. C* **82** (2022) 661 [[2204.05024](#)].
- [46] K.S. Babu, S. Jana and V.P. K., *Correlating W -Boson Mass Shift with Muon $g-2$ in the Two Higgs Doublet Model*, *Phys. Rev. Lett.* **129** (2022) 121803 [[2204.05303](#)].
- [47] R. Balkin, E. Madge, T. Menzo, G. Perez, Y. Soreq and J. Zupan, *On the implications of positive W mass shift*, *JHEP* **05** (2022) 133 [[2204.05992](#)].
- [48] Y.H. Ahn, S.K. Kang and R. Ramos, *Implications of New CDF-II W Boson Mass on Two Higgs Doublet Model*, *Phys. Rev. D* **106** (2022) 055038 [[2204.06485](#)].
- [49] J. Kawamura, S. Okawa and Y. Omura, *W boson mass and muon $g-2$ in a lepton portal dark matter model*, *Phys. Rev. D* **106** (2022) 015005 [[2204.07022](#)].
- [50] A. Ghoshal, N. Okada, S. Okada, D. Raut, Q. Shafi and A. Thapa, *Type III seesaw with R -parity violation in light of m_W (CDF)*, [2204.07138](#).
- [51] S. Kanemura and K. Yagyu, *Implication of the W boson mass anomaly at CDF II in the Higgs triplet model with a mass difference*, *Phys. Lett. B* **831** (2022) 137217 [[2204.07511](#)].
- [52] T.A. Chowdhury, J. Heeck, A. Thapa and S. Saad, *W boson mass shift and muon magnetic moment in the Zee model*, *Phys. Rev. D* **106** (2022) 035004 [[2204.08390](#)].
- [53] D. Borah, S. Mahapatra and N. Sahu, *Singlet-doublet fermion origin of dark matter, neutrino mass and W -mass anomaly*, *Phys. Lett. B* **831** (2022) 137196 [[2204.09671](#)].
- [54] S. Lee, K. Cheung, J. Kim, C.-T. Lu and J. Song, *Status of the two-Higgs-doublet model in light of the CDF m_W measurement*, *Phys. Rev. D* **106** (2022) 075013 [[2204.10338](#)].
- [55] H. Abouabid, A. Arhrib, R. Benbrik, M. Krab and M. Ouchemhou, *Is the new CDF M_W measurement consistent with the two higgs doublet model?*, [2204.12018](#).
- [56] J. Kim, S. Lee, P. Sanyal and J. Song, *CDF W -boson mass and muon $g-2$ in a type- X two-Higgs-doublet model with a Higgs-phobic light pseudoscalar*, *Phys. Rev. D* **106** (2022) 035002 [[2205.01701](#)].
- [57] T.A. Chowdhury and S. Saad, *Leptoquark-vectorlike quark model for the CDF m_W , $(g-2)_\mu$, $RK^{(*)}$ anomalies, and neutrino masses*, *Phys. Rev. D* **106** (2022) 055017 [[2205.03917](#)].
- [58] S. Hossenfelder, S. Hossenfelder and W. Hollik, *Two-loop improved predictions for M_W and $\sin^2\theta_{\text{eff}}$ in Two-Higgs-Doublet models*, *Eur. Phys. J. C* **82** (2022) 970 [[2207.03845](#)].
- [59] B.D. Sáez and K. Ghorbani, *Singlet scalars as dark matter and the muon $(g - 2)$ anomaly*, *Phys. Lett. B* **823** (2021) 136750 [[2107.08945](#)].

- [60] N. Chakrabarty, I. Chakraborty, D.K. Ghosh and G. Saha, *Muon $g - 2$ and W -mass in a framework of colored scalars: an LHC perspective*, [2212.14458](#).
- [61] P. Agrawal, D.E. Kaplan, O. Kim, S. Rajendran and M. Reig, *Searching for axion forces with precision precession in storage rings*, [2210.17547](#).
- [62] N. Chakrabarty, *The muon $g - 2$ and W -mass anomalies explained and the electroweak vacuum stabilised by extending the minimal Type-II seesaw*, [2206.11771](#).
- [63] W. Abdallah, R. Gandhi and S. Roy, *LSND and MiniBooNE as guideposts to understanding the muon $g - 2$ results and the CDF II W mass measurement*, [2208.02264](#).
- [64] J.J. Heckman, *Extra W -boson mass from a $D3$ -brane*, *Phys. Lett. B* **833** (2022) 137387 [[2204.05302](#)].
- [65] G. Hiller, C. Hormigos-Feliu, D.F. Litim and T. Steudtner, *Anomalous magnetic moments from asymptotic safety*, *Phys. Rev. D* **102** (2020) 071901 [[1910.14062](#)].
- [66] X.-F. Han, T. Li, L. Wang and Y. Zhang, *Simple interpretations of lepton anomalies in the lepton-specific inert two-Higgs-doublet model*, *Phys. Rev. D* **99** (2019) 095034 [[1812.02449](#)].
- [67] A.R. Zhitnitsky, *On Possible Suppression of the Axion Hadron Interactions. (In Russian)*, *Sov. J. Nucl. Phys.* **31** (1980) 260.
- [68] M. Dine, W. Fischler and M. Srednicki, *A Simple Solution to the Strong CP Problem with a Harmless Axion*, *Phys. Lett. B* **104** (1981) 199.
- [69] PARTICLE DATA GROUP collaboration, *Review of Particle Physics*, *Chin. Phys. C* **38** (2014) 090001.
- [70] CMS collaboration, *Search for an exotic decay of the Higgs boson to a pair of light pseudoscalars in the final state of two muons and two τ leptons in proton-proton collisions at $\sqrt{s} = 13$ TeV*, *JHEP* **11** (2018) 018 [[1805.04865](#)].
- [71] G.G. Raffelt, *Astrophysical axion bounds*, *Lect. Notes Phys.* **741** (2008) 51 [[hep-ph/0611350](#)].
- [72] A. Arvanitaki, S. Dimopoulos, S. Dubovsky, N. Kaloper and J. March-Russell, *String Axiverse*, *Phys. Rev. D* **81** (2010) 123530 [[0905.4720](#)].
- [73] J.E. Kim, *Weak Interaction Singlet and Strong CP Invariance*, *Phys. Rev. Lett.* **43** (1979) 103.
- [74] M.A. Shifman, A.I. Vainshtein and V.I. Zakharov, *Can Confinement Ensure Natural CP Invariance of Strong Interactions?*, *Nucl. Phys. B* **166** (1980) 493.
- [75] M. Ahmadvand, *Filtered asymmetric dark matter during the Peccei-Quinn phase transition*, *JHEP* **10** (2021) 109 [[2108.00958](#)].
- [76] D. Espriu, F. Mescia and A. Renau, *Axion-Higgs interplay in the two Higgs-doublet model*, *Phys. Rev. D* **92** (2015) 095013 [[1503.02953](#)].
- [77] G.C. Branco, P.M. Ferreira, L. Lavoura, M.N. Rebelo, M. Sher and J.P. Silva, *Theory and phenomenology of two-Higgs-doublet models*, *Phys. Rept.* **516** (2012) 1 [[1106.0034](#)].
- [78] MSSM WORKING GROUP collaboration, *The Minimal supersymmetric standard model: Group summary report*, in *GDR (Groupement De Recherche) - Supersymetrie*, 12, 1998 [[hep-ph/9901246](#)].
- [79] ALEPH, DELPHI, L3, OPAL, LEP collaboration, *Search for Charged Higgs bosons: Combined Results Using LEP Data*, *Eur. Phys. J. C* **73** (2013) 2463 [[1301.6065](#)].

- [80] CDF collaboration, *Search for charged Higgs bosons in decays of top quarks in p anti- p collisions at $\sqrt{s} = 1.96$ TeV*, *Phys. Rev. Lett.* **103** (2009) 101803 [[0907.1269](#)].
- [81] LHC HIGGS CROSS SECTION WORKING GROUP collaboration, *Handbook of LHC Higgs Cross Sections: 4. Deciphering the Nature of the Higgs Sector*, [1610.07922](#).
- [82] T. Ahmed, M. Bonvini, M.C. Kumar, P. Mathews, N. Rana, V. Ravindran et al., *Pseudo-scalar Higgs boson production at N^3 LO_A + N^3 LL'*, *Eur. Phys. J. C* **76** (2016) 663 [[1606.00837](#)].
- [83] M.E. Peskin and T. Takeuchi, *A New constraint on a strongly interacting Higgs sector*, *Phys. Rev. Lett.* **65** (1990) 964.
- [84] M.E. Peskin and T. Takeuchi, *Estimation of oblique electroweak corrections*, *Phys. Rev. D* **46** (1992) 381.
- [85] K. Ghorbani and P. Ghorbani, *W-boson mass anomaly from scale invariant 2HDM*, *Nucl. Phys. B* **984** (2022) 115980 [[2204.09001](#)].
- [86] R. Foot, A. Kobakhidze, K.L. McDonald and R.R. Volkas, *Poincaré protection for a natural electroweak scale*, *Phys. Rev. D* **89** (2014) 115018 [[1310.0223](#)].
- [87] H.H. Patel, *Package-X: A Mathematica package for the analytic calculation of one-loop integrals*, *Comput. Phys. Commun.* **197** (2015) 276 [[1503.01469](#)].
- [88] A. Keshavarzi, K.S. Khaw and T. Yoshioka, *Muon $g - 2$: A review*, *Nucl. Phys. B* **975** (2022) 115675 [[2106.06723](#)].
- [89] S.M. Barr and A. Zee, *Electric Dipole Moment of the Electron and of the Neutron*, *Phys. Rev. Lett.* **65** (1990) 21.
- [90] V. Ilisie, *New Barr-Zee contributions to $(g - 2)_\mu$ in two-Higgs-doublet models*, *JHEP* **04** (2015) 077 [[1502.04199](#)].
- [91] A. Chierchia, P. Kneschke, D. Stöckinger and H. Stöckinger-Kim, *The muon magnetic moment in the 2HDM: complete two-loop result*, *JHEP* **01** (2017) 007 [[1607.06292](#)].
- [92] A. Broggio, E.J. Chun, M. Passera, K.M. Patel and S.K. Vempati, *Limiting two-Higgs-doublet models*, *JHEP* **11** (2014) 058 [[1409.3199](#)].
- [93] A. Jueid, J. Kim, S. Lee and J. Song, *Type-X two-Higgs-doublet model in light of the muon $g-2$: Confronting Higgs boson and collider data*, *Phys. Rev. D* **104** (2021) 095008 [[2104.10175](#)].
- [94] F.J. Botella, F. Cornet-Gomez, C. Miró and M. Nebot, *Muon and electron $g - 2$ anomalies in a flavor conserving 2HDM with an oblique view on the CDF M_W value*, *Eur. Phys. J. C* **82** (2022) 915 [[2205.01115](#)].
- [95] MEG collaboration, *Search for the lepton flavour violating decay $\mu^+ \rightarrow e^+ \gamma$ with the full dataset of the MEG experiment*, *Eur. Phys. J. C* **76** (2016) 434 [[1605.05081](#)].